NJC

View Online
Dynamic Article Links

Cite this: *New J. Chem.*, 2011, **35**, 1596–1606

www.rsc.org/njc

PAPER

Dialkoxy functionalized quaternary ammonium ionic liquids as potential electrolytes and cellulose solvents

Zhengjian Chen,[ab] Shimin Liu,[a] Zuopeng Li,[a] Qinghua Zhang[a] and Youquan Deng*[a]

Received (in Montpellier, France) 25th January 2011, Accepted 18th April 2011
DOI: 10.1039/c1nj20062c

A series of new ionic liquids, based on dialkoxy-functionalized quaternary ammonium cations {side chains: 1 = CH_3, 1O1 = CH_3OCH_2, 1O2 = $CH_3OC_2H_4$, 2O2 = $C_2H_5OC_2H_4$; cations: $[N_{11,1O1,1O2}]$, $[N_{11,1O1,2O2}]$, $[N_{11,1O2,1O2}]$, $[N_{11,1O2,2O2}]$ and $[N_{11,2O2,2O2}]$}, with BF_4^-, $(CF_3SO_2)_2N^-$ (NTf_2) and $CH_3CO_2^-$ (OAc) as counteranions, have been prepared and characterized. Their basic properties, such as spectroscopic characteristics, melting point, glass transition temperature, thermal stability, electrochemical window, density, refractive index, viscosity and conductivity, were measured and comparatively studied. The incorporation of two flexible alkoxy chains makes the quaternary ammonium salts highly qualified to be low-viscous and high-conductive room temperature ILs, and even some of them have significantly better fluidity than the popular imidazolium ILs with a similar molecular weight, *e.g.* $[N_{11,1O1,2O2}]BF_4$ (151 cP and 2.11 mS cm^{-1}, M_w: 249) *vs.* $[HMIm]BF_4$ (220 cP and 1.2 mS cm^{-1}, M_w: 256) at 25 °C. The electrochemical windows of these ILs were evaluated up to 5.5 V. In addition, the dialkoxy OAc ILs were found to have excellent solvent power for cellulose under mild conditions, *e.g.* a solution of 18 wt% microcrystalline cellulose in $[N_{11,2O2,2O2}]$OAc at 80 °C. By precipitation with water, the dissolved cellulose (I crystal structure) was regenerated as nanosized cellulose II particles with increased surface area and decreased crystallinity, determined by FE-SEM and XRD.

Introduction

Ionic liquids (ILs), a class of modern solvents, are of increasing interest because of their versatile applications in various fields: organic synthesis,[1] transition metal catalysis,[2] biotechnology,[3] separation techniques,[4] ionothermal synthesis,[5] nano-materials,[6] lubricants,[7] lithium-ion batteries,[8] dye-sensitized solar cells,[9] supercapacitors,[10] sensors,[11] light-emitting materials,[12] magnetic fluids,[13] and so on. The major advantage of ILs is their superior physicochemical properties, including negligible vapor pressure that offers the greatest environmental benefit, low flammability, wide liquid range, high conductivity and wide electrochemical window and so on. Additionally, the structures and properties of ILs can be custom-tailored to fit each specific purpose, through incorporating anions or cations with functional groups, such as $-NH_2$,[14] –COOH,[15] $-SO_3H$,[16] –OH,[17] –CN,[18] and –SH,[19] *etc.*, which provides more promising perspectives in both fundamental and practical aspects. However, functionalized ILs are usually much more viscous than their non-functionalized analogues, since the incorporation of any functional group will inevitably lead to an increase in both polarity and molecular size. In many fields, the required viscosity of ILs should be as low as possible, including heterogeneous catalysis and supporting electrolytes, but except viscous lubricants.

Among various types of functional groups, alkoxy groups are exceptionally featured by their ability to form low-viscosity ILs, since the highly flexible alkoxy chains do not pack as efficiently as alkyl chains, according to molecular dynamics simulations.[20] Up to now, ether-functionalized ILs have included imidazolium cations,[21–26] quaternary ammonium cations,[20,27–31] phosphonium cations,[32] cyclic quaternary ammonium cations,[33,34] guanidinium cations,[35,36] sulfonium cations,[37] as well as perfluoroalkylborate anions.[38] As a matter of fact, the alkoxy chain effect on viscosity strongly depends on the IL structure, and for example prefers to be present in quaternary ammonium ILs rather than in imidazolium ILs.[21,27] The poor alkoxy chain effect on viscosity reduction of imidazolium ILs may be related to the hydrogen bonds between alkoxy oxygen atoms and imidazolium ring hydrogen atoms,[22] leading to reduced flexibility of alkoxy groups. In contrast, the alkoxy chains in quaternary ammonium ILs can be flexible enough to remarkably reduce viscosity, relative to isoelectronic alkyl chains.[20] As a result,

[a] *Centre for Green Chemistry and Catalysis, Lanzhou Institute of Chemical Physics, Chinese Academy of Sciences, Lanzhou, 730000, China. E-mail: ydeng@licp.cas.cn; Fax: +86-931-4968116*
[b] *Graduate School of the Chinese Academy of Sciences, Beijing 100039, China*

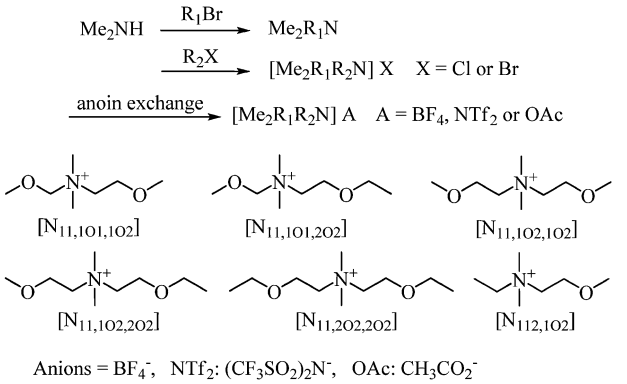

Scheme 1 Structures and abbreviations of the cations and anions used in this work.

the alkoxy-functionalized quaternary ammonium ILs have been used as high-conductivity electrolytes in electrochemical devices.[28,29]

Recently, ILs have also shown significant promise in biomass processing, in particular cellulose.[39–41] Cellulose is the most abundant renewable natural polymer that can be converted into value-added fuels and chemicals.[39–43] However, one of the main barriers to the use of cellulose is its poor solubility in organic solvents, due to its strong hydrogen-bonding network and high crystallinity.[44,45] Recently, ILs were reported to be effective in dissolving cellulose, especially for those with strong hydrogen-bond accepting anions, such as Cl^-,[46,47] $Me_2PO_4^-$,[48] HCO_2^-,[49] and $CH_3CO_2^-$,[50] *etc*. These anions can interact with hydroxyl groups and disrupt the hydrogen bonds in cellulose.[51,52] For example, solutions of up to 25 wt% cellulose were prepared in [BMIm]Cl under microwave heating.[46] Moreover, the methods to convert cellulose, such as direct hydrolysis to hydroxymethylfurfural,[53] hydrogenation to hexitols,[54] and acetylation of cellulose,[55] *etc*., have been successfully performed in ILs. Another alternative to the use of ILs for cellulose is pretreatment, since the dissolved cellulose can be easily regenerated by precipitation with water or organic solvents.[56,57] The regenerated cellulose is less crystalline than the native ones, providing greater accessibility to chemical and enzymatic transformations.[57,58]

Although ether groups have been shown to exert a favourable effect on increasing the fluidity of ILs, there is little information about di- or multi-ether functionalized ILs, except for dialkoxy imidazolium ILs[23] and poly(ethylene glycol)-ammonium ILs.[31] Therefore, it is still unknown whether the alkoxy chain effect on fluidity persists in ILs with more than one ether group attached, and how other properties of these ILs will be. To answer these questions, this paper introduces and characterizes a new class of dialkoxy functionalized quaternary ammonium ILs (Scheme 1).

Results and discussion

Synthesis and characterization

Scheme 1 outlines the three-step synthesis of the new dialkoxy-functionalized quaternary ammonium ILs. First, tertiary amines ($Me_2NC_2H_4OCH_3$ and $Me_2NC_2H_4OC_2H_5$) were synthesized from the alkylation reaction between $HN(CH_3)_2$ and $BrC_2H_4OCH_3$ or $BrC_2H_4OC_2H_5$. Then the tertiary amines were quaternized with different alkoxyalkyl halides to yield ammonium halide salts. In the final step, anion exchange reaction afforded the desired ILs. For comparisons, monoalkoxy [$N_{112,1O2}$] ILs were also prepared. These newly prepared compounds were confirmed by ^{1}H-NMR, FT-IR, ESI-MS (positive ion mode), ion-selective electrodes and moisture meter. The observed spectral data are well consistent with the expected structure and composition. The residual halide ion concentrations in halide-free salts were evaluated to be less than 0.26%. The water content could be reduced to 40–70 ppm for NTf_2 ILs, 80–120 ppm for BF_4 ILs, and 200–300 ppm for OAc ILs, after vacuum drying for 24 h at 80 °C and 10^{-2}–10^{-3} mbar. This vacuum drying process would be carried out again, prior to each property test.

The thermal properties, such as melting point, glass transition temperature, crystallization temperature, solid–solid transition temperature and thermal stability of these (di)alkoxy Ils, were investigated using differential scanning calorimetry (DSC) and thermogravimetry (DTA). For BF_4- and NTf_2-based salts, which are liquids at room temperature, their basic properties, such as density, refractive index, electrochemical window, viscosity and conductivity, were measured and comparatively studied. Besides, the dialkoxy OAc ILs were found to have excellent performance in dissolving cellulose. The regenerated cellulose samples were characterized by field emission scanning electron microscopy (FE-SEM) and X-ray diffraction (XRD).

Phase transition and melting point

The solid–liquid phase transition of these ILs was determined by differential scanning calorimetry (DSC). The corresponding data for glass-transition temperature (T_g), crystallization temperature (T_c), melting point (T_m) and solid–solid transition temperature (T_{s-s}) are summarized in Table 1.

In general, four types of phase transition behaviors could be observed for all of these ILs during a cooling and heating

Table 1 Thermal properties of the (di)alkoxy ILs[a]

Entry	IL	T_g[b]/°C	T_c[c]/°C	T_m[d]/°C	T_{s-s}[e]/°C
1	[$N_{112,1O2}$]BF_4	−94.0[f]	(−43.5)[g]	7.8[h]	
2	[$N_{11,1O1,1O2}$]BF_4	−91.0			
3	[$N_{11,1O1,2O2}$]BF_4	−89.6			
4	[$N_{11,1O2,1O2}$]BF_4		−32.8	35.9	
5	[$N_{11,1O2,2O2}$]BF_4	−79.0	(−18.8)	6.4	
6	[$N_{11,2O2,2O2}$]BF_4	−80.5			
7	[$N_{112,1O2}$]NTf_2	−95.6[i]			
8	[$N_{11,1O1,1O2}$]NTf_2	−90.4			
9	[$N_{11,1O1,2O2}$]NTf_2	−89.8			
10	[$N_{11,1O2,1O2}$]NTf_2	−82.3			
11	[$N_{11,1O2,2O2}$]NTf_2	−84.3			
12	[$N_{11,2O2,2O2}$]NTf_2	−84.8			
13	[$N_{112,1O2}$]OAc		22.0	36.1	
14	[$N_{11,1O2,1O2}$]OAc		27.1	39.7	
15	[$N_{11,1O2,2O2}$]OAc	−58.8	(−19.5)	31.1	3.4, 20.3
16	[$N_{11,2O2,2O2}$]OAc		3.2	34.3	−26.9, −8.9, 23.2

[a] At a scanning rate of 10 °C min^{-1}, except for OAc-based salts at 5 °C min^{-1}. [b] Glass-transition temperature. [c] Crystallization temperature upon cooling (upon heating). [d] Melting point. [e] Solid–solid transition temperature. [f] Literature value: −97.27 [g] Literature value: −26.27 [h] Literature value: 4.27 [i] Literature value: −96.27

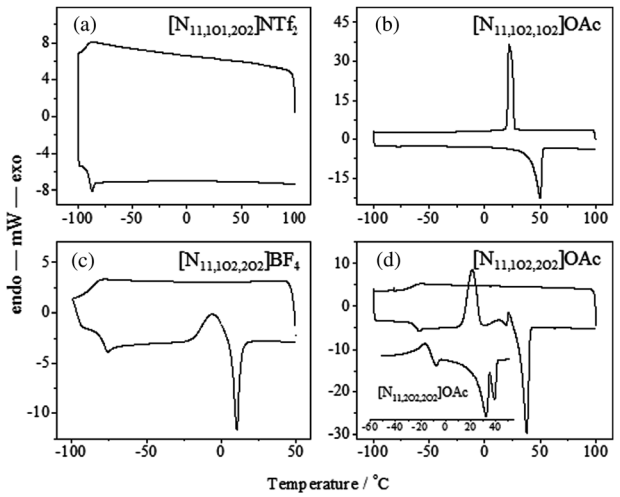

Fig. 1 Different phase transition behaviors of the (di)alkoxy ILs.

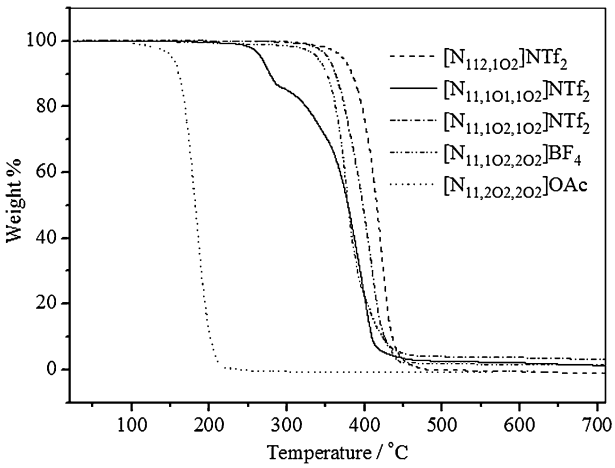

Fig. 2 TGA traces of five ILs.

cycle (Fig. 1). The first type shows only liquid–glass transition without freezing and melting (Fig. 1a, entries 2, 3 and 6–12 in Table 1). In addition to some BF_4-based salts, all of the NTf_2 salts engage in this behavior. In our opinion, the highly flexible alkoxy groups and the NTf_2 anion that has two co-conformations[59] reduce the packing efficiency of ILs and allow them to form an amorphous glass rather than an ordered crystalline solid at low temperature. The second type is characteristic of a fast crystallization process upon cooling, followed by a melting point upon heating (Fig. 1b, entries 4, 13 and 14 in Table 1). Two dialkoxy ILs engaging in this behavior are both based on the symmetrical $[N_{11,1O2,1O2}]$ cation (with BF_4 and OAc), arguing for the promotion function of the cation symmetry on the crystallization of ILs. The third type is represented by two low-symmetry salts, such as $[N_{11,1O2,2O2}]BF_4$ that shows cold crystallization between its glass transition point and melting point (Fig. 1c, entries 1 and 5, Table 1). The fourth type is characteristic of polymorphic transitions (Fig. 1d, entries 15 and 16 in Table 1). For example, $[N_{11,1O2,2O2}]$OAc underwent two exothermic solid–solid transitions at 3.4 and 20.3 °C to the stable state prior to final melting at 31.1 °C. Besides, a large enthalpy gain, generally referred to as a plastic crystal,[60] was observed at 23.2 °C for $[N_{11,2O2,2O2}]$OAc.

Seven of the 16 ILs were shown to have melting points (T_ms) below 39.7 °C (entries 1, 4, 5 and 13–16 in Table 1). The melting point reflects the strength of a crystal lattice that is governed by three major factors: intermolecular force, molecular symmetry and the degree of conformational freedom.[61] For a given anion (BF_4 or OAc), the T_m values of ILs decrease in the order: $[N_{11,1O2,1O2}] > [N_{112,1O2}] > [N_{11,1O2,2O2}]$, for example, $[N_{11,1O2,1O2}]BF_4$ (35.9 °C), $[N_{112,1O2}]BF_4$ (7.8 °C) and $[N_{11,1O2,2O2}]BF_4$ (6.4 °C). In this order, the lowest T_m value is expected for $[N_{11,1O2,2O2}]$-containing salts, because $[N_{11,1O2,2O2}]$ is less symmetrical than $[N_{11,1O2,1O2}]$ and is richer in side-chain conformations than $[N_{112,1O2}]$. Consequently, the second alkoxy chain was found to be able to decrease the melting points of quaternary ammonium ILs, though only in the case of different chain lengths. Generally, BF_4-based salts exhibit lower melting points than their OAc counterparts. The negative charge delocalization of the BF_4 anion over the four electronegative F atoms should be responsible for the lower melting points of BF_4 ILs, through weakening cation–anion interaction.[1]

Table 2 Thermal decomposition temperature (T_d) of nine ILs

Entry	ILs	T_d[a]/°C
1	$[N_{112,1O2}]BF_4$	376[b]
2	$[N_{11,1O1,1O2}]BF_4$	245
3	$[N_{11,1O1,2O2}]BF_4$	243
4	$[N_{11,1O2,2O2}]BF_4$	339
5	$[N_{112,1O2}]NTf_2$	387[c]
6	$[N_{11,1O1,1O2}]NTf_2$	266
7	$[N_{11,1O2,1O2}]NTf_2$	351
8	$[N_{112,1O2}]$OAc	160
9	$[N_{11,2O2,2O2}]$OAc	151

[a] Temperature at 5% mass loss. [b] Literature value 377 °C.[27] [c] Literature value 388 °C.[27]

Thermal stability

The thermal stability of nine ILs, which cover all kinds of ions used in this paper, was determined by thermogravimetry (TGA). Fig. 2 shows five typical TGA curves, and Table 2 presents the corresponding thermal decomposition temperature (T_d), ranging from 151 to 387 °C. The observed DTA results reflect that the thermal stability of these salts depends on the substituent group electronegativity and the anion nucleophilicity, referring to the nucleophilic N^+-dealkylation mechanism for IL thermolysis.[62]

On the one hand, incorporating a second ether group exerts a negative effect on the thermal stability of ILs, in particular a 1O1 group with a short spacer length of only one methylene between the alkoxy oxygen atom and the quaternary nitrogen atom, for example (T_d), $[N_{112,1O2}]BF_4$ (376 °C) > $[N_{11,1O2,2O2}]BF_4$ (339 °C) ≫ $[N_{11,1O1,1O2}]BF_4$ (245 °C). As could be deduced from the ^{1}H-NMR spectra (δ ppm, see Experimental section), where (*e.g.*, in Fig. 3) the proton chemical shifts of $-OCH_3$ (3.38 and 3.67 ppm) are greater than that of $-N^+CH_3$ (3.12 ppm), the alkoxy oxygen atom tends to be a bit more electronegative than the quaternary nitrogen atom. Thus, the electron-withdrawing nature of alkoxy

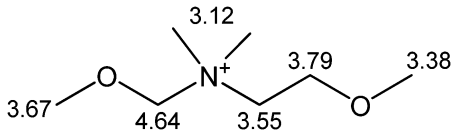

Fig. 3 The proton chemical shifts (δ ppm) of $[N_{11,1O1,1O2}]BF_4$ in CCl_3D.

groups should be considered in making the cation more sensitive to the nucleophilic attack of anion on heating, *via* increasing the positive charge density on the cation core. This proposition was also supported by the oxygen-induced δ increase in the $-N^+CH_2R$ moiety, which denotes the electron-withdrawing ability of ether groups. For example, the δ values in the N^+-bound methylene: $N^+CH_2CH_3$ (3.55 ppm, in $[N_{112,1O2}]BF_4$) < $N^+CH_2CH_2OCH_2CH_3$ (3.65 ppm, in $[N_{11,1O2,2O2}]BF_4$) ≪ $N^+CH_2OCH_3$ (4.64 ppm, in $[N_{11,1O1,1O2}]BF_4$), correlate well with the above T_d order, in turn from 376 °C to 339 °C and to 245 °C.

On the other hand, the anion species also shows a significant effect on the thermal stability of ILs. As might be expected, the ILs with the weakly nucleophilic BF_4 and NTf_2 anions[62] exhibit much better thermal stability than OAc ILs. For example, the T_d values of the three $[N_{112,1O2}]$ derivatives are, respectively, 376 °C for BF_4, 387 °C for NTf_2 and only 160 °C for OAc.

Electrochemical window

A wide electrochemical window is required for ILs to be used as electrolytes in electrochemical devices, like capacitor or battery systems with high energy and power density.[63] One of the most attractive properties of quaternary ammonium ILs is their high electrochemical stability in comparison with imidazolium ILs.[27] The electrochemical windows of the room-temperature ILs used in this paper were evaluated by cyclic voltammetry on a glassy-carbon electrode, as illustrated in Fig. 4. Table 3 shows the test results for the respective cathodic ($E_{cathodic}$) and anodic (E_{anodic}) limits, and electrochemical windows (EW = $E_{anodic} - E_{cathodic}$). Evidently, all of the measured ILs possess wide electrochemical windows, ranging up to 5.30–5.57 V. Unlike the first alkoxy group (sometimes causes more than 0.5 V reduction in EW),[27,34] the second alkoxy group shows no significant negative effect on the electrochemical windows of the dialkoxy ILs. Consequently, the electrochemical stability of these ILs is comparable to that of tetraalkylammonium ILs (~5.6 V)[1,27,38] and pyrrolidinium ILs (~5.5 V),[34,63,64] and is larger than imidazolium ILs (~4.5 V)[21,65] and protic ILs (~4.0 V).[66] Sometimes, the

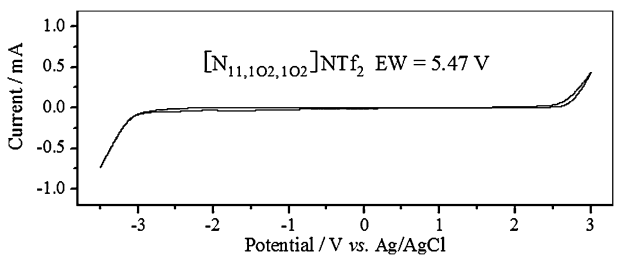

Fig. 4 Typical cyclic voltammetry of $[N_{11,1O2,1O2}]NTf_2$.

Table 3 Cathodic and anodic limits ($E_{cathodic}$ and E_{anodic} *vs.* Ag/AgCl) and electrochemical windows (EW) for the (di)alkoxy ILs based on BF_4 and NTf_2, determined on a glassy carbon electrode at room temperature

Entry	ILs	$E_{cathodic}$/V	E_{anodic}/V	EW/V
1	$[N_{112,1O2}]BF_4$	−2.94	2.45	5.39
2	$[N_{11,1O1,1O2}]BF_4$	−2.95	2.35	5.30
3	$[N_{11,1O1,2O2}]BF_4$	−3.11	2.30	5.41
4	$[N_{11,1O2,1O2}]BF_4$[a]	−2.90	2.43	5.33
5	$[N_{11,1O2,2O2}]BF_4$	−2.91	2.42	5.33
6	$[N_{11,2O2,2O2}]BF_4$	−2.98	2.36	5.34
7	$[N_{112,1O2}]NTf_2$	−2.95	2.59	5.54[b]
8	$[N_{11,1O1,1O2}]NTf_2$	−3.07	2.49	5.56
9	$[N_{11,1O1,2O2}]NTf_2$	−3.08	2.49	5.57
10	$[N_{11,1O2,1O2}]NTf_2$	−2.95	2.52	5.47
11	$[N_{11,1O2,2O2}]NTf_2$	−3.03	2.45	5.48
12	$[N_{11,2O2,2O2}]NTf_2$	−2.95	2.48	5.43

[a] Being supercooled for about 0.5 h at 25 °C. [b] Literature value 5.40 V.[27]

Table 4 Some basic properties of the (di)alkoxy ILs based on BF_4 and NTf_2 at 25 °C

Entry	IL	ρ[b]/g cm^{-3}	n[c]	η[d]/cP	κ[e]/mS cm^{-1}
1	$[N_{112,1O2}]BF_4$	1.1952[f]	1.3980	308[g]	1.78[h]
2	$[N_{11,1O1,1O2}]BF_4$	1.2321	1.3985	171	2.20
3	$[N_{11,1O1,2O2}]BF_4$	1.1894	1.4007	151	2.11
4	$[N_{11,1O2,1O2}]BF_4$[a]	1.2115	1.4086	338	1.03
5	$[N_{11,1O2,2O2}]BF_4$	1.1730	1.4094	274	1.04
6	$[N_{11,2O2,2O2}]BF_4$	1.1418	1.4096	223	1.02
7	$[N_{112,1O2}]NTf_2$	1.4318[i]	1.4104	61.2[j]	3.14[k]
8	$[N_{11,1O1,1O2}]NTf_2$	1.4466	1.4098	49.5	3.46
9	$[N_{11,1O1,2O2}]NTf_2$	1.4054	1.4095	47.9	3.21
10	$[N_{11,1O2,1O2}]NTf_2$	1.4215	1.4147	66.9	2.45
11	$[N_{11,1O2,2O2}]NTf_2$	1.3819	1.4143	63.4	2.30
12	$[N_{11,2O2,2O2}]NTf_2$	1.3475	1.4139	58.6	2.18

[a] Being supercooled for about 0.5 h at 25 °C. [b] Density. [c] Refractive index. [d] Viscosity. [e] Conductivity. [f] Literature value 1.21.[27] [g] Literature value 335.[27] [h] Literature value 1.7.[27] [i] Literature value 1.45.[27] [j] Literature value 60.[27] [k] Literature value 3.1.[27]

second alkoxy group can even enhance the cathodic limit, for example, $[N_{112,1O2}]BF_4$ ($E_{cathodic}$ = −2.94 V) *vs.* $[N_{11,1O1,2O2}]BF_4$ ($E_{cathodic}$ = −3.11 V). In the surroundings of the dialkoxy cations, both BF_4 and NTf_2 have high anodic stability with E_{anodic} = 2.45 ± 0.15 V.

Density and refractive index

Physicochemical properties, including density, refractive index, viscosity and conductivity of these (di)alkoxy ILs based on BF_4 and NTf_2 at 25 °C were investigated, as summarized in Table 4. Fig. 5 presents the obtained density (ρ, Table 4) values at 25 °C, ranging from 1.1418 to 1.4466 g mL^{-1}. In comparison to $[N_{112,1O2}]$ ILs, $[N_{11,1O1,1O2}]$ analogues are a bit more dense, as a result of incorporating an additional alkoxy oxygen unit. For the dialkoxy ILs, their density shows a general decrease with lengthening of the alkoxy chains, *i.e.* $[N_{11,1O1,1O2}] > \{[N_{11,1O2,1O2}] > [N_{11,1O1,2O2}]\} > [N_{11,1O2,2O2}] > [N_{11,2O2,2O2}]$. However, although $[N_{11,1O2,1O2}]$ and $[N_{11,1O1,2O2}]$ are structurally similar isomers, the former ILs are comparatively more dense (about 0.02 g mL^{-1}) than the latter ILs, *e.g.*, $[N_{11,1O2,1O2}]BF_4$ (1.2115 g mL^{-1}) *vs.* $[N_{11,1O1,2O2}]BF_4$ (1.1894 g mL^{-1}) at 25 °C. This finding can

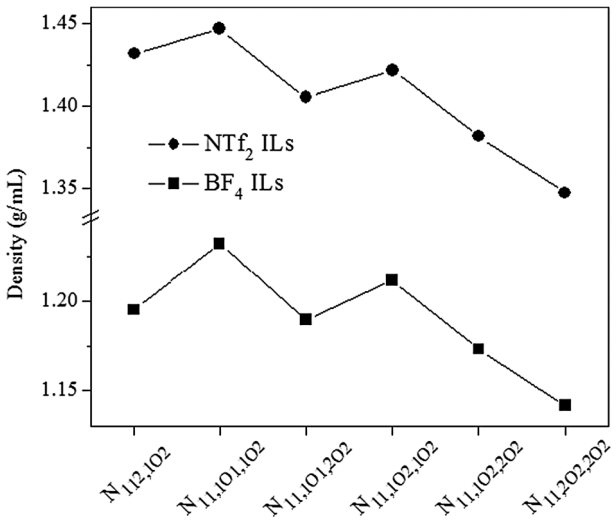

Fig. 5 Density of the (di)alkoxy ILs based on BF_4 and NTf_2 at 25 °C.

be extended to account for the great difference in refractive index, viscosity and conductivity between these isomeric ILs (see below). Besides, NTf_2-based ILs ($\sim$1.4 g mL^{-1}) are much more dense than BF_4 ILs ($\sim$1.2 g mL^{-1}), mainly because of the heavy sulfur in NTf_2.

The refractive index (n, Table 4) of these (di)alkoxy ILs (BF_4 and NTf_2) at 25 °C lies in a range of 1.3980–1.4147. As seen in Fig. 6, the anion species (BF_4 and NTf_2), the incorporation of an alkoxy oxygen atom {[$N_{112,1O2}$] *vs.* [$N_{11,1O1,1O2}$]}, and the alkoxy chain length (1O1, 1O2 and 2O2) all have but little impact ($< \pm 0.01$) on the refractive index. According to the Lorenz–Lorentz equation:

$$(n^2 - 1)/(n^2 - 1) = 4\pi\rho Na/3M$$

where ρ is the density, N is a constant, a is the polarizability and M is the molar mass, respectively, the refractive index generally increases with increasing polarizability and density.[67] High polarizability implies great electron-cloud deformability. The strong electron-withdrawing fluorine atoms "lock up" the electron clouds of the perfluorinated anions (BF_4 and NTf_2), and lead the ILs to show low refractive index ($<$1.415). In Fig. 6, only a small change in refractive index occurs during gradually lengthening the alkoxy chains. Interestingly, there is a comparatively large difference in the refractive index between the isomeric ILs. For a given anion, the refractive index of [$N_{11,1O2,1O2}$] ILs is larger than that of [$N_{11,1O1,2O2}$] ILs, which results from the above-mentioned fact that the former are more dense than the latter.

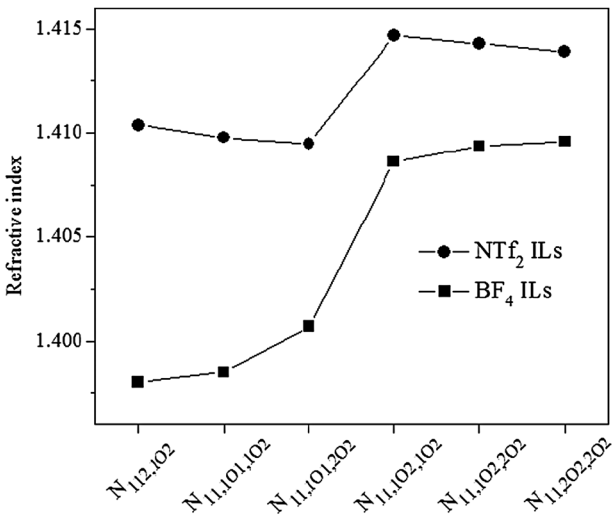

Fig. 6 Refractive index of the (di)alkoxy ILs based on BF_4 and NTf_2 at 25 °C.

Viscosity

Viscosity is an important parameter for ILs in determining their potential for applications, because low viscosity is required for high conductivity and a fast mass transport rate, and to facilitate operations, like filtration, extraction and decantation. Relative to imidazolium ILs, quaternary ammonium ILs are usually rather viscous, which limits their applications, especially in the field of electrochemistry, in spite of their high electrochemical stability. Although many quaternary ammonium ILs with a flexible ether bond have been shown to own low viscosity, they are still more viscous than their imidazolium analogues.[34] One of the purposes in this work is to test the feasibility of providing lower-viscous quaternary ammonium ILs, through incorporating more than one alkoxy group.

The viscosity (η, Table 4) values of these (di)alkoxy ILs (BF_4 and NTf_2) were plotted in Fig. 7, ranging from 47.9 to 338 cP at 25 °C. The evidence derived from the η values confirms that the second alkoxy group can further markedly decrease the viscosity of quaternary ammonium ILs, for example, [$N_{11,1O1,1O2}$]BF_4 (171 cP) is only half as viscous as [$N_{112,1O2}$]BF_4 (308 cP) at 25 °C. In addition, some of these dialkoxy quaternary ammonium ILs are even evidently less viscous than imidazolium ILs with a similar molecular weight, *e.g.*, [$N_{11,1O1,2O2}$]BF_4 (151 cP, M_w: 249) *vs.* 1-hexyl-3-methylimidazolium [HMIm]BF_4 (220 cP, M_w: 256)[21] at 25 °C. For a constant anion, the viscosity of these dialkoxy ILs decreases in the following order: {[$N_{11,1O2,1O2}$] > [$N_{11,1O2,2O2}$] > [$N_{11,2O2,2O2}$] > [$N_{11,1O1,1O2}$] > [$N_{11,1O1,2O2}$]}. In this order, the η values fail to increase with lengthening of side chain,

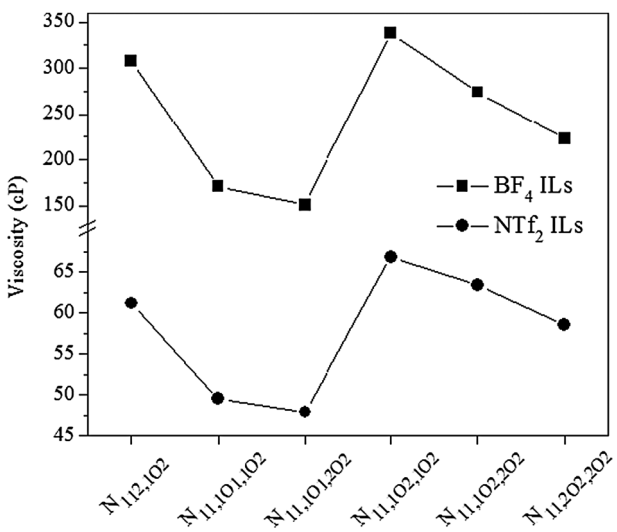

Fig. 7 Viscosity of the (di)alkoxy ILs based on BF_4 and NTf_2 at 25 °C.

Table 5 Temperature-dependent viscosity and Arrhenius parameters

η/cP				
°C\IL	$[N_{11,1O2,2O2}]OAc$	$[N_{11,1O2,2O2}]BF_4$	$[N_{11,1O1,2O2}]NTf_2$	$[N_{112,1O2}]NTf_2$
25	930	274	47.9	61.2
30	661	193	39.4	53.1
40	315	112	27.1	37.0
50	158	71.1	19.4	25.1
60	89.0	46.0	14.5	18.4
70	49.1	31.4	11.6	14.0
80	32.2	23.3	9.2	11.1
$\ln\eta = \ln A + E_\eta/RT$ (T in K, R = 8.314 J mol^{-1} K^{-1})				
E_η[a]/kJ mol^{-1}	54.6	39.2	26.4	28.0
A/cP	2.6×10^{-7}	3.5×10^{-5}	1.1×10^{-3}	7.8×10^{-4}
R^2[b]	0.9993	0.9980	0.9983	0.9990

[a] Activation energy. [b] Linear fitting parameter.

as usual.[68] In brief, the contribution of each alkoxy group to viscosity follows the order of (1O2 > 2O2 > 1O1). The (1O2 > 2O2) relation on viscosity argues that the 2O2 group is longer but more flexible than the 1O2 group, and flexibility dominates over length in reducing the viscosity of the ether derivatives. Another interesting feature in Fig. 7 is that among the ILs with a common anion, the most and the least viscous ones are, respectively, based on $[N_{11,1O2,1O2}]$ and $[N_{11,1O1,2O2}]$, although they are isomers of each other. A possible explanation for the distinct difference in viscosity between the isomeric ILs is their unequal densities, as mentioned above. In detail, the less dense $[N_{11,1O1,2O2}]$ ILs, relative to $[N_{11,1O2,1O2}]$ ILs, pack loosely with more interstices to promote mass transport, by referring to the hole theory.[69] Besides, the anion species plays an important role in determining the viscosity of ILs, and generally follows the order of OAc > BF_4 > NTf_2, in agreement with the previous literature.[68] For example, three $[N_{11,1O2,2O2}]$-based salts are, respectively, 930 cP for OAc, 274 cP for BF_4 and 63.4 cP for NTf_2, at 25 °C.

The temperature dependence of viscosity was investigated for four ILs over a temperature range from 25 to 80 °C, as listed in Table 5. The viscosity of the four ILs decreases with increasing temperature, as usual.[70] However, there is a great difference in the decreasing rate of viscosity among these ILs. Generally, the more viscous ILs decrease more rapidly in viscosity. For example, the viscosity of $[N_{11,1O2,2O2}]$OAc could be decreased 28.9 times from 930 to 32.2 cP, and yet $[N_{11,1O1,2O2}]NTf_2$ was decreased only 5.2 times from 47.9 to 9.2 cP, when heated from 25 to 80 °C. The Arrhenius plots of viscosity were also constructed according to the equation:

$$\ln\eta = \ln A + E_\eta/RT$$

as illustrated in Fig. 8. The values of E_η, A, and the linear fitting parameter (R^2) for the ILs were calculated and listed in Table 5. According to the values of R^2 (>0.99), these ILs were well fit with the Arrhenius model from 25 to 80 °C. E_η is the activation energy for viscous flow, which is always regarded as the energy barrier to be overcome by ion transport. Among the four ILs, the E_η value decreases in the order: $[N_{11,1O2,2O2}]$OAc (54.6 kJ mol^{-1}) > $[N_{11,1O2,2O2}]BF_4$ (39.2 kJ mol^{-1}) > $[N_{112,1O2}]NTf_2$ (28.0 kJ mol^{-1}) > $[N_{11,1O1,2O2}]NTf_2$ (26.4 kJ mol^{-1}). This evidence indicates that the NTf_2 ILs have a lower energy barrier and therefore show lower viscosity and slower decreasing rate of viscosity.

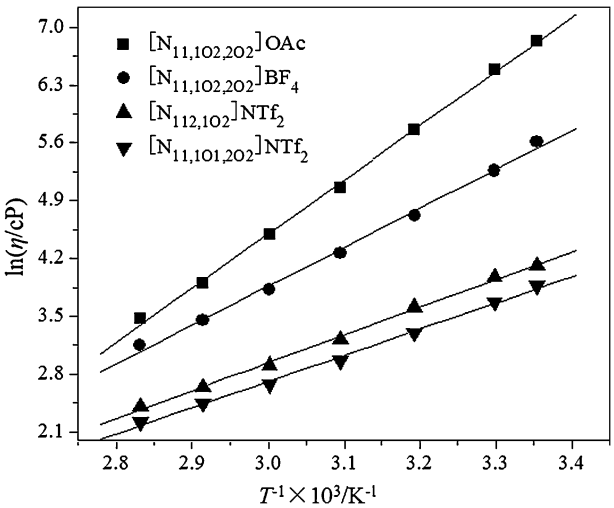

Fig. 8 Arrhenius plots of viscosity for four ILs.

Conductivity

Low viscosity allows high conductivity for ILs to be applied as electrolytes in electrochemical devices. Another major factor on conductivity of ILs is the ionic volume. Fig. 9 summarizes the conductivity (κ, Table 4) of the (di)alkoxy ILs based on BF_4 and NTf_2 at 25 °C, varying in a range from 1.02 to 3.46 mS cm^{-1}. In comparison to $[N_{112,1O2}]$-based ILs, although $[N_{11,1O1,1O2}]$ ILs are larger with an additional alkoxy oxygen atom, they still display higher conductivity, owing to their lower viscosity, for example, $[N_{112,1O2}]BF_4$ (1.78 mS cm^{-1}) *vs.* $[N_{11,1O1,1O2}]BF_4$ (2.20 mS cm^{-1}) at 25 °C. Additionally, some of the dialkoxy ILs can be even more conductive than imidazolium ILs of a similar molecular weight, for example, $[N_{11,1O1,2O2}]BF_4$ (2.11 mS cm^{-1}) *vs.* [HMIm]BF_4 (1.2 mS cm^{-1})[21] at 25 °C. Keeping the anion constant, these ILs {*e.g.*, $[N_{11,1O1,1O2}]NTf_2$: 3.46 mS cm^{-1}, 25 °C} are also more conductive than tetraalkylammonium, pyrrolidinium and protic ILs, such as $[N_{1116}]NTf_2$ (0.43 mS cm^{-1}, 25 °C),[71] $[P_{14}]NTf_2$ (2.2 mS cm^{-1}, 25 °C),[64] and triethylammonium NTf_2 (3.2 mS cm^{-1}, 130 °C),[72] but less conductive than [ethyl-MIm]-based ILs, such as [EMIm]NTf_2 (8.8 mS cm^{-1}, 20 °C)[65] and

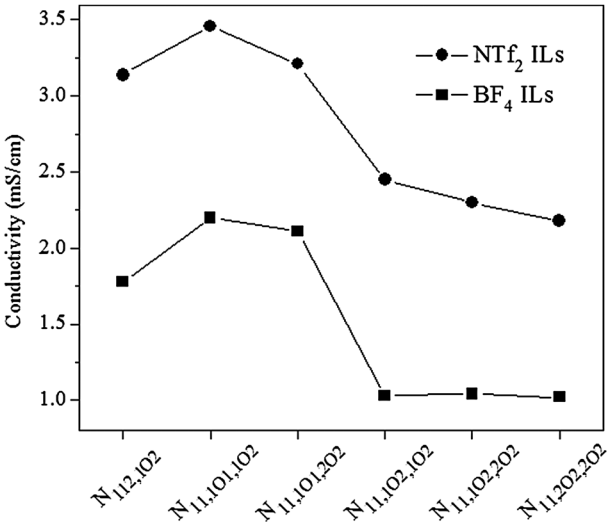

Fig. 9 Conductivity of the (di)alkoxy ILs based on BF_4 and NTf_2 at 25 °C.

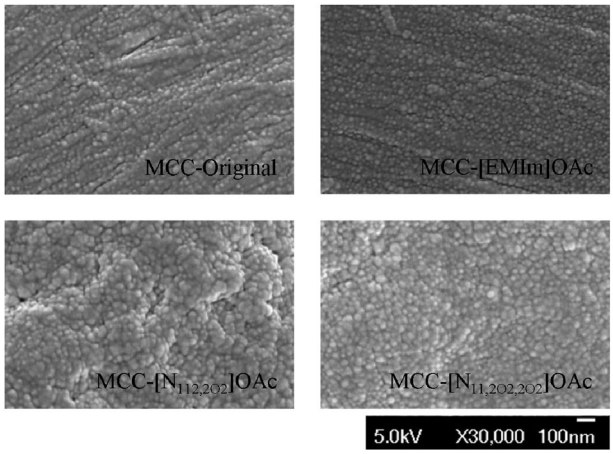

Fig. 10 FE-SEM images of the original and IL-treated cellulose samples.

[EMIm]BF_4 (13.6 mS cm^{-1}, 25 °C).[21] For a common anion, the conductivity of the dialkoxy ILs generally decreases in the order of {[$N_{11,1O1,1O2}$] ≥ [$N_{11,1O1,2O2}$] > [$N_{11,1O2,1O2}$] ≥ [$N_{11,1O2,2O2}$] ≥ [$N_{11,2O2,2O2}$]}, which can be briefed as group contribution: (1O1 > 1O2 ≥ 2O2). This order is determined by two major factors: alkoxy chain length (2O2 > 1O2 > 1O1) and the above-mentioned viscosity order (1O2 > 2O2 > 1O1). For the isomeric ILs, viscosity is the only decisive factor on their conductivity. As a result, [$N_{11,1O1,2O2}$]BF_4 (2.11 mS cm^{-1} and 151 cP) can be twice more conductive than [$N_{11,1O2,1O2}$]BF_4 (1.03 mS cm^{-1} and 338 cP) at 25 °C.

Dissolution of microcrystalline cellulose

These dialkoxy ILs ought to be cellulose-philic, in virtue of the hydrogen bond acceptor at the alkoxy oxygen unit. Thereby, we tested their performance in dissolving microcrystalline cellulose (MCC with a degree of polymerization: 215–240). The solubility (wt%, Table 6) of MCC in ILs was determined by addition of MCC in small batches at 80 °C. As is evident from the obtained results, the solvent power of the dialkoxy OAc ILs (15–18 wt%) for MCC is powerful, comparing favourably with [EMIm]OAc (17 wt%), and other effective IL solvents for cellulose, such as [butyl-MIm]Cl (10 wt%, 100 °C, DP = 1000;[46] 18 wt%, 83 °C, DP = 286)[73] and [allyl-MIm]Cl (14.5 wt%, 80 °C, DP = 225).[47] The relatively low solubility of MCC in [$N_{112,1O2}$]OAc (13 wt%) indicates that the ether group is helpful for ILs to dissolve cellulose. Among the three dialkoxy ILs, [$N_{11,2O2,2O2}$]OAc (18 wt%) is the most efficient solvent for cellulose, followed by [$N_{11,1O2,2O2}$]OAc (17 wt%) and [$N_{11,1O2,1O2}$]OAc (15 wt%). Generally, high anion concentration can make for high solvent power for cellulose.[52] However, the OAc concentration order of {[$N_{11,2O2,2O2}$]OAc < [$N_{11,1O2,2O2}$]OAc < [$N_{11,1O2,1O2}$]OAc} goes against their solvent power for cellulose, in turn from 18 wt% to 17 wt% to 15 wt%. This finding might be better understood in conjunction with the spatial heterogeneity in IL with an amphiphilic cation due to the aggregation of alkyl tails.[74,75] The hydrophobic tail aggregation implies a trend to make other parts more hydrophilic and polar. Hence, an appropriate increase in alkoxy chains leads ILs to be more powerful cellulose solvents, through increasing the spatial heterogeneity. The ILs with BF_4 and NTf_2 (entries 6 and 7, Table 6) are poor solvents for MCC, consistent with previous reports.[52]

Table 6 Solubility of MCC in ILs at 80 °C

Entry	IL	Solubility of MCC at 80 °C (wt%)
1	[$N_{11,1O2,1O2}$]OAc	15
2	[$N_{11,1O2,2O2}$]OAc	17
3	[$N_{11,2O2,2O2}$]OAc	18
4	[$N_{112,1O2}$]OAc	13
5	[EMIm]OAc[a]	17
6	[$N_{11,1O2,1O2}$]BF_4	No sol.[b]
7	[$N_{11,1O2,2O2}$]NTf_2	No sol.[b]

[a] 1-Ethyl-3-methylimidazolium OAc. [b] Solubility < 1 wt%.

In order to evaluate the influence of IL treatment on the cellulose structure, 5 wt% MCC/IL solutions were employed to regenerate MCC by precipitation with distilled water and drying *in vacuo*. The regenerated MCCs were characterized using field emission scanning electron microscopy (FE-SEM) and X-ray diffraction (XRD). As shown in Fig. 10, the IL-treated MCCs have different surface morphologies from the original sample, where the linear fibrils reflect the nature of the linear cellulose molecules.[76] The MCC regenerated from [EMIm]OAc also shows linear textures, similar to the original MCC but smaller in size. Meanwhile, the alkoxy quaternary ammonium ILs transform the dissolved MCC into nanosized cellulose particles. Relative to the [$N_{112,1O2}$]OAc-treated MCC, the [$N_{11,2O2,2O2}$]OAc-treated MCC seems smaller-sized in dimension, implying a larger accessible surface area for reagents to react with.[77] Fig. 11 shows XRD patterns of different cellulose samples. The original MCC displays a typical cellulose I structure with five diffraction peaks at 14.9°, 16.6°, 20.6°, 22.8° and 34.5°, assigned respectively to (101), (10$\bar{1}$), (021), (002) and (040).[45] After IL treatment, the cellulose II pattern was obtained, where three peaks at 12.1°, 20.2° and 21.5° can be indexed as the (101), (10$\bar{1}$) and (002) reflections of the cellulose II structure.[78] The integral area of the XRD curves

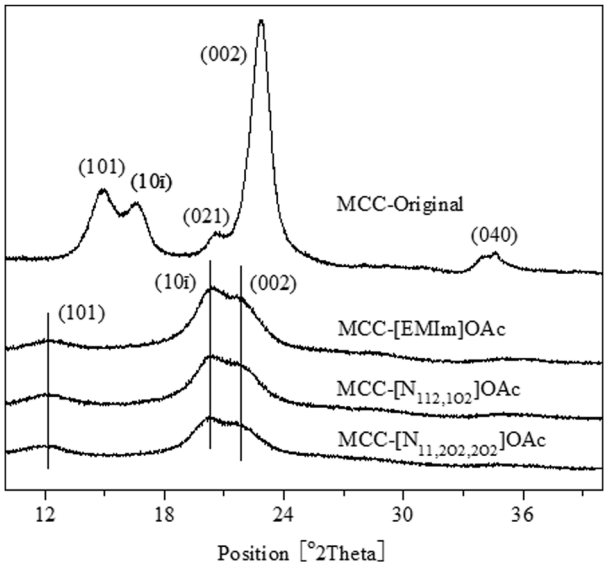

Fig. 11 XRD patterns of the original and IL-treated cellulose samples.

was calculated to be 1.62, 1.41, 1.15 for the MCCs from [EMIm]OAc, $[N_{112,1O2}]$OAc and $[N_{11,2O2,2O2}]$OAc, respectively. As a result, the $[N_{11,2O2,2O2}]$OAc-treated MCC has the lowest crystallinity, suggesting promise in cellulose pretreatment.

Conclusions

This paper presents a new class of diether-substituted quaternary ammonium ILs {side chains: 1 = CH_3, 1O1 = CH_3OCH_2, 1O2 = $CH_3OC_2H_4$, 2O2 = $C_2H_5OC_2H_4$; ions: $[N_{11,1O1,1O2}]$, $[N_{11,1O1,2O2}]$, $[N_{11,1O2,1O2}]$, $[N_{11,1O2,2O2}]$, $[N_{11,2O2,2O2}]$; counter-anions: BF_4^-, $(CF_3SO_2)_2N^-$ (NTf_2) and $CH_3CO_2^-$ (OAc)}. Their basic physicochemical properties, such as spectroscopic characteristics, crystallization temperature, melting point, glass transition temperature, solid–solid transition temperature, thermal stability, electrochemical window, density, refractive index, viscosity and conductivity were measured and comparatively studied with the monoalkoxy $[N_{112,1O2}]$-based ILs. Most of the (di)alkoxy quaternary ammonium salts are liquid at room temperature. The ILs bearing two different alkoxy groups tend to have a low or non-existent melting point (<31.1 °C). The dialkoxy ILs exhibit lower thermal stability (151–351 °C) than $[N_{112,1O2}]$ salts (160–387 °C), due to the electron-withdrawing nature of alkoxy groups. The ILs based on BF_4 and NTf_2 have wide electrochemical windows of up to 5.30–5.57 V, suffering no significant negative impact from the combination of a second alkoxy group. Due to the presence of two flexible alkoxy chains, the dialkoxy quaternary ammonium salts are well qualified to be low-viscous and high-conductive ILs (minimum to 47.9 cP and maximum to 3.46 mS cm^{-1} at 25 °C), and even some of them are not only much more fluid than $[N_{112,1O2}]$ ILs, but also more than imidazolium ILs with a similar molecular weight. The dialkoxy OAc ILs are effective in dissolving cellulose (up to 18 wt% at 80 °C), with the help of the hydrogen accepting ether bonds. Hence, the dialkoxy functionalized quaternary ammonium ILs could be promising as both electrolytes and cellulose solvents.

Experimental section

^{1}H-NMR, FT-IR, ESI-MS and GC/MS

^{1}H-NMR spectra (δ, ppm) were determined on a Mercury Plus spectrometer (400 MHz). FT-IR spectra (cm^{-1}) were obtained in KBr discs using a Nicolet 5700 FT-IR spectrophotometer. ESI-MS spectra (positive ion mode, m/z) were measured in methanol on a Bruker Daltonics APEX II 47e FTMS. The GC/MS (m/z) analyses were conducted with an Agilent 5973 mass selective detector/6890 GC/data system.

Water content and halide content

After vacuum drying at 80 °C and 10^{-2}–10^{-3} mbar for 24 h, the water content of each IL sample was determined by Karl-Fischer titration, by using a Metrohm 831 KF Coulometer. The residual halide content in halide-free ILs was evaluated by ion-selective electrodes (Cl^- and Br^-).

Phase transition and thermal stability

The solid–liquid phase transition was investigated on a Mettler Toledo differential scanning calorimeter model DSC822^e, on a cooling and heating cycle at a scanning rate of 10 °C min^{-1}, except for OAc-based ILs at 5 °C min^{-1}. The thermal stability study was recorded with 5 wt% of mass loss on a Pyris Diamond Perkin-Elmer TG/DTA at a rate of 10 °C min^{-1} under an N_2 atmosphere.

Density, refractive index, viscosity and conductivity

The density was determined using a volume–mass method in a 10 mL volumetric flask calibrated with water. The refractive index measurement was conducted on a WAY-2s Abbe refractometer. The viscosity was determined on a Stabinger Viscosimeter SVM 3000/GR. The conductivity was obtained using a Mettler-Toledo Seven Multimeter. The temperature for the measurements was maintained at 25 ± 0.1 °C by means of an external temperature controller.

Electrochemical window

The cyclic voltammetry testing was carried out on a CHI 660A Electrochemical Work Station with a glassy carbon working electrode and an Ag wire pseudo reference electrode at room temperature.

Dissolution and regeneration of cellulose

The solubility of cellulose was determined by increasing the cellulose concentration by 1.0 wt% increment. The mixture was heated at 80 °C and stirred under a nitrogen atmosphere in a glove box. Incremental cellulose was added until the solution became optically transparent. The saturation point was considered to be reached when cellulose could not be dissolved again within 5 h. The regeneration of cellulose was performed on a 0.5 g scale. In a typical experiment, 50 mL distilled water was added to a 5 wt% cellulose/IL solution (10 g) at room temperature, and vigorously stirred for 2 h. The cellulose suspension was filtered and washed with running distilled water and acetone (5 × 20 mL). Then the regenerated cellulose was dried under vacuum for 24 h at room temperature.

FE-SEM and XRD

The surface morphologies of cellulose samples were determined by field emission scanning electron microscopy (FE-SEM, JSM-6701F). X-Ray diffraction (XRD) was measured using a Siemens D/max-RB powder X-ray diffractometer. The diffraction patterns were recorded with Cu Kα radiation (40 mA, 40 kV) over a 2θ range from 10° to 80° and a position-sentient detector.

Synthesis of $[N_{11,1O2}]$. $CH_3OC_2H_4Br$ (185.2 g, 1.33 mol) was added dropwise to 33% aqueous dimethylamine solution (546 g, 4.0 mol) and stirred for 24 h at 40 °C. After stirring, the mixture was neutralized by 2 M aqueous NaOH (1.33 mol), and then an appropriate amount of NaCl was dissolved to make a saturated solution. Then the solution was azeotropically distilled with the fraction collected between 80 and 90 °C. The collected fraction was dried over KOH pellets, filtered and washed with anhydrous diethyl ether (5 × 100 mL). Subsequent fractional distillation of the dried solution gave the product as a colorless liquid (bp: 96–98 °C, 86 g, yield: 63%). GC/MS: m/z = 15, 30, 42, 58, 72, 103.

Synthesis of $[N_{11,2O2}]$. The alkylation reaction, neutralization and saturation followed the same procedure as described in the synthesis of $[N_{11,1O2}]$, except that $C_2H_5OC_2H_4Br$ was used instead of $CH_3OC_2H_4Br$. The saturated solution was extracted with diethyl ether (5 × 100 mL). The collected extracts were dried with KOH pellets, filtered and rinsed with anhydrous diethyl ether (3 × 100 mL). Then, fractional distillation of the dried solution gave the target product as a colorless liquid (bp: 116–118 °C, 97 g, yield: 62%). GC/MS: m/z = 15, 30, 42, 58, 72, 117.

Synthesis of $[N_{11,1O1,1O2}]$Cl and $[N_{11,1O1,2O2}]$Cl. CH_3OCH_2Cl (30.1 mL, 0.40 mol) was added dropwise to a mixture of 60 mL anhydrous dichloromethane and $[N_{11,1O2}]$ or $[N_{11,2O2}]$ (0.40 mol equiv.) in a round bottom flask fitted with a drying tube at 0 °C. After stirring for 4 h at 30 °C, the solvent was evaporated under vacuum at 50 °C, affording the desired product as a pale yellow viscous liquid (yield > 99%).

Synthesis of $[N_{11,1O2,1O2}]$Br, $[N_{11,1O2,2O2}]$Br, $[N_{11,2O2,2O2}]$Br and $[N_{112,1O2}]$Br. In a typical procedure, a tertiary amine {$[N_{11,1O2}]$ or $[N_{11,2O2}]$} (0.40 mol) was put into acetonitrile (80 mL) and the appropriate alkyl or alkoxyalkyl bromide (0.44 mol) was added. After stirring for 48 h at 40 °C, the solvent was removed under vacuum at 80 °C, leaving a pale yellow solid. Recrystallization from a mixture of acetone and anhydrous diethyl ether afforded a white solid (yield ≈ 90%).

Synthesis of NTf_2 ILs. In a typical procedure, an ammonium halide (0.10 mol) and lithium bis(trifluoromethylsulfonyl)-imide ($LiNTf_2$) (0.12 mol) were added into 50 mL distilled water and stirred for 4 h at room temperature. After the reaction, the upper water phase was decanted off. The bottom IL phase was washed three times with distilled water (20 mL) in a separating funnel. Concentration under vacuum at 80 °C yielded a colorless or pale yellow liquid.

$[N_{11,1O1,1O2}]NTf_2$. Pale yellow liquid; yield: 88%; water content: 66 ppm; chloride ion concentration: 0.02 wt%; ^{1}H-NMR (CCl_3D, 400 MHz, ppm): 4.58 (s, 2H), 3.77 (t, 2H), 3.66 (s, 3H), 3.52 (t, 2H), 3.39 (s, 3H), 3.10 (s, 6H); IR (cm^{-1}): 2950, 2904, 2838, 1476, 1353, 1194, 1138, 1057; ESI-MS (m/z): 148.1336 for $[N_{11,1O1,1O2}]^+$ with a calculated value of 148.13.

$[N_{11,1O1,2O2}]NTf_2$. Pale yellow liquid; yield: 90%; water content: 63 ppm; chloride ion concentration: 0.03 wt%; ^{1}H-NMR (CCl_3D, 400 MHz, ppm): 4.60 (s, 2H), 3.81 (t, 2H), 3.66 (s, 3H), 3.60 (t, 2H), 3.54 (q, 2H), 3.11 (s, 6H), 1.21 (t, 3H); IR (cm^{-1}): 2981, 2938, 2881, 1474, 1352, 1190, 1135, 1055; ESI-MS (m/z): 162.1493 for $[N_{11,1O1,2O2}]^+$ with a calculated value of 162.15.

$[N_{11,1O2,1O2}]NTf_2$. Colorless liquid; yield: 89%; water content: 51 ppm; bromide ion concentration: 0.01 wt%; ^{1}H-NMR (CCl_3D, 400 MHz, ppm): 3.79 (t, 4H), 3.62 (t, 4H), 3.38 (s, 6H), 3.20 (s, 6H); IR (cm^{-1}): 2942, 2900, 2831, 1477, 1352, 1192, 1136, 1056; ESI-MS (m/z): 162.1492 for $[N_{11,1O2,1O2}]^+$ with a calculated value of 162.15.

$[N_{11,1O2,2O2}]NTf_2$. Colorless liquid; yield: 91%; water content: 46 ppm; bromide ion concentration: 0.01 wt%; ^{1}H-NMR (CCl_3D, 400 MHz, ppm): 3.82 (m, 4H), 3.62 (m, 4H), 3.53 (q, 2H), 3.38 (s, 3H), 3.21 (s, 6H), 1.20 (t, 3H), 1.22 (m, 3H); IR (cm^{-1}): 2982, 2938, 2888, 2830, 1476, 1351, 1190, 1134, 1054; ESI-MS (m/z): 176.1644 for $[N_{11,1O2,2O2}]^+$ with a calculated value of 176.16.

$[N_{11,2O2,2O2}]NTf_2$. Colorless liquid; yield: 89%; water content: 48 ppm; bromide ion concentration: 0.01 wt%; ^{1}H-NMR (CCl_3D, 400 MHz, ppm): 3.84 (m, 4H), 3.62 (m, 4H), 3.53 (m, 4H), 3.21 (s, 6H), 1.20 (m, 3H), 1.20 (m, 6H); IR (cm^{-1}): 2981, 2937, 2878, 1476, 1351, 1188, 1134, 1055; ESI-MS (m/z): 190.1806 for $[N_{11,2O2,2O2}]^+$ with a calculated value of 190.18.

$[N_{112,1O2}]NTf_2$. Colorless liquid; yield: 92%; water content: 65 ppm; bromide ion concentration: 0.02 wt%; ^{1}H-NMR (CCl_3D, 400 MHz, ppm): 3.79 (t, 2H), 3.52 (t, 2H), 3.48 (q, 2H), 3.38 (s, 3H), 3.10 (s, 6H), 1.40 (t, 3H); IR (cm^{-1}): 2946, 2899, 2830, 1485, 1353, 1196, 1139, 1057.

Synthesis of BF_4 ILs. The anion exchange was performed by using triethyloxonium tetrafluoroborate {$[Et_3O]BF_4$}, which was prepared following a published method.[79] In a typical procedure, an ammonium halide (0.10 mol) and equimolar $[Et_3O]BF_4$ were added to 40 mL anhydrous dichloromethane in a round bottom flask equipped with a drying tube. After stirring for 2 h at room temperature, the mixture was concentrated *in vacuo* at 80 °C to remove the solvent, yielding a colorless or pale yellow liquid.

$[N_{11,1O1,1O2}]BF_4$. Pale yellow liquid; yield > 99%; water content: 112 ppm; chloride ion concentration: 0.12 wt%; ^{1}H-NMR (CCl_3D, 400 MHz, ppm): 4.64 (s, 2H), 3.79 (t, 2H), 3.67 (s, 3H), 3.55 (t, 2H), 3.38 (s, 3H), 3.12 (s, 6H); FT-IR (cm^{-1}): 2951, 2907, 2837, 1636, 1479, 1410, 1286, 1205, 1120, 1055.

$[N_{11,1O1,2O2}]BF_4$. Pale yellow liquid; yield > 99%; water content: 106 ppm; chloride ion concentration: 0.12 wt%; ^{1}H-NMR (CCl_3D, 400 MHz, ppm): 4.66 (s, 2H), 3.82 (t, 2H), 3.67 (s, 3H), 3.54 (t, 2H), 3.53 (q, 2H), 3.13 (s, 6H),

1.20 (t, 3H); FT-IR (cm^{-1}): 2979, 2937, 2879, 1637, 1480, 1389, 1203, 1119, 1055.

[$N_{11,1O2,1O2}$]BF_4. Colorless liquid that crystallized at ambient temperature; yield > 99%; water content: 95 ppm; bromide ion concentration: 0.15 wt%; ^{1}H-NMR (CCl_3D, 400 MHz, ppm): 3.81 (t, 4H), 3.64 (t, 4H), 3.37 (s, 6H), 3.22 (s, 6H); FT-IR (cm^{-1}): 2993, 2942, 2903, 2830, 1636, 1480, 1410, 1286, 1200, 1121, 1058.

[$N_{11,1O2,2O2}$]BF_4. Colorless liquid; yield > 99%; water content: 93 ppm; bromide ion concentration: 0.18 wt%; ^{1}H-NMR (CCl_3D, 400 MHz, ppm): 3.84 (m, 4H), 3.65 (m, 4H), 3.53 (q, 2H), 3.38 (s, 3H), 3.23 (s, 6H), 1.19 (t, 3H). FT-IR (cm^{-1}): 2979, 2936, 2890, 1637, 1481, 1379, 1285, 1201, 1120, 1055.

[$N_{11,2O2,2O2}$]BF_4. Colorless liquid; yield > 99%; water content: 88 ppm; bromide ion concentration: 0.15 wt%; ^{1}H-NMR (CCl_3D, 400 MHz, ppm): 3.85 (t, 4H), 3.66 (t, 4H), 3.53 (q, 4H), 3.24 (s, 6H), 1.19 (t, 6H); FT-IR (cm^{-1}): 2978, 2935, 2876, 1638, 1485, 1379, 1285, 1221, 1124, 1055.

[$N_{112,1O2}$]BF_4. Colorless liquid; yield > 99%; water content: 102 ppm; bromide ion concentration: 0.12 wt%; ^{1}H-NMR (CCl_3D, 400 MHz, ppm): 3.81 (t, 2H), 3.55 (t, 2H), 3.50 (q, 2H), 3.38 (s, 3H), 3.15 (s, 6H), 1.40 (t, 3H); FT-IR (cm^{-1}): 2995, 2948, 2903, 2830, 1636, 1401, 1487, 1286, 1191, 1056.

Synthesis of OAc ILs. In a typical procedure, an ammonium halide (0.15 mol) was dissolved in distilled water (300 mL) and freshly prepared silver acetate (AgOAc) (0.18 mol) was added. After vigorous stirring for 5 h at room temperature, the mixture was filtrated and washed with distilled water (3 × 100 mL). The filtrate was collected and concentrated under vacuum at 80 °C, yielding the desired product.

[$N_{11,1O2,1O2}$]OAc. Pale yellow liquid that crystallized at room temperature; yield: 84%; water content: 224 ppm; bromide ion concentration: 0.22 wt%; ^{1}H-NMR (CCl_3D, 400 MHz, ppm): 3.90 (t, 4H), 3.65 (t, 4H), 3.40 (s, 6H), 3.19 (s, 6H), 1.92 (s, 3H); FT-IR (cm^{-1}): 3005, 2979, 2814, 1655, 1567, 1477, 1406, 1122, 1032.

[$N_{11,1O2,2O2}$]OAc. Pale yellow liquid that crystallized at room temperature; yield: 82%; water content: 255 ppm; bromide ion concentration: 0.14 wt%; ^{1}H-NMR (CCl_3D, 400 MHz, ppm): 3.94 (t, 2H), 3.90 (t, 2H), 3.63 (m, 6H), 3.40 (s, 3H), 3.20 (s, 6H), 1.92 (s, 3H), 1.21 (t, 3H); IR (cm^{-1}): 2979, 2942, 2900, 2834, 1645, 1567, 1478, 1406, 1120, 1021.

[$N_{11,2O2,2O2}$]OAc. Pale yellow liquid that crystallized at room temperature; yield: 80%; water content: 266 ppm; bromide ion concentration: 0.26 wt%; ^{1}H-NMR (CCl_3D, 400 MHz, ppm): 3.95 (t, 4H), 3.64 (m, 8H), 3.21 (s, 6H), 1.92 (s, 3H), 1.21 (t, 6H); IR (cm^{-1}): 2978, 2934, 2883, 1653, 1569, 1484, 1405, 1121, 1048.

[$N_{112,1O2}$]OAc. Pale yellow liquid that crystallized at room temperature; yield: 83%; water content: 298 ppm; bromide ion concentration: 0.17 wt%; ^{1}H-NMR (CCl_3D, 400 MHz, ppm): 3.89 (t, 2H), 3.55 (t, 2H), 3.46 (q, 2H), 3.40 (s, 3H), 3.10 (s, 6H), 1.92 (s, 3H), 1.36 (t, 3H); IR (cm^{-1}): 2997, 2942, 2831, 1648, 1557, 1484, 1406, 1116, 1021.

Acknowledgements

We acknowledge the National Natural Science Foundation of China (No. 20533080) for financial support.

Notes and references

1 P. Wasserscheid and T. Welton, *Ionic Liquids in Synthesis*, 2nd edn, Wiley-VCH, Weinheim, 2008.
2 P. Wasserscheid and W. Keim, *Angew. Chem., Int. Ed.*, 2000, **39**, 3772.
3 C. Roosen, P. Müller and L. Greiner, *Appl. Microbiol. Biotechnol.*, 2008, **81**, 607.
4 D. Han and K. H. Row, *Molecules*, 2010, **15**, 2405.
5 E. R. Parnham and R. E. Morris, *Acc. Chem. Res.*, 2007, **40**, 1005.
6 K. Okazaki, T. Kiyama, K. Hirahara, N. Tanaka, S. Kuwabata and T. Torimoto, *Chem. Commun.*, 2008, 691.
7 F. Zhou, Y. Liang and W. Liu, *Chem. Soc. Rev.*, 2009, **38**, 2590; I. Minami, *Molecules*, 2009, **14**, 2286; M.-D. Bermúdez, A.-E. Jiménez, J. Sanes and F.-J. Carrión, *Molecules*, 2009, **14**, 2888.
8 A. Lewandowski and A. Świderska-Mocek, *J. Power Sources*, 2009, **194**, 601.
9 N. Cai, J. Zhang, D. Zhou, Z. Yi, J. Guo and P. Wang, *J. Phys. Chem. C*, 2009, **113**, 4215.
10 D. Wei and T. W. Ng, *Electrochem. Commun.*, 2009, **11**, 1996.
11 L. C. Branco and F. Pina, *Chem. Commun.*, 2009, 6204.
12 S. Tang, A. Babai and A.-V. Mudring, *Angew. Chem., Int. Ed.*, 2008, **120**, 7631.
13 T. Peppel, M. Köckerling, M. Geppert-Rybczyńska, R. V. Ralys, J. K. Lehmann, S. P. Verevkin and A. Heintz, *Angew. Chem., Int. Ed.*, 2010, **49**, 7116.
14 H. Yu, Y.-T. Wu, Y.-Y. Jiang, Z. Zhou and Z.-B. Zhang, *New J. Chem.*, 2009, **33**, 2385.
15 P. Nockemann, R. V. Deun, B. Thijs, D. Huys, E. Vanecht, K. V. Hecke, L. V. Meervelt and K. Binnemans, *Inorg. Chem.*, 2010, **49**, 3351.
16 J. Akbari, A. Heydari, H. R. Kalhor and S. A. Kohan, *J. Comb. Chem.*, 2010, **12**, 137.
17 J. Y. Z. Chiou, J. N. Chen, J. S. Lei and I. J. B. Lin, *J. Mater. Chem.*, 2006, **16**, 2972.
18 A. I. Siriwardana, A. A. J. Torriero, J. M. Reyna-Gonzlez, I. M. Burgar, N. F. Dunlop, A. M. Bond, G. B. Deacon and D. R. MacFarlane, *J. Org. Chem.*, 2010, **75**, 8376.
19 G. Fang, J. Zhang, J. Lu, L. Ma and S. Wang, *Microchim. Acta*, 2010, **171**, 305.
20 L. J. A. Siqueira and M. C. C. Ribeiro, *J. Phys. Chem. B*, 2009, **113**, 1074.
21 Z.-B. Zhou, H. Matsumoto and K. Tatsumi, *Chem.–Eur. J.*, 2004, **10**, 6581.
22 Z. Fei, W. H. Ang, D. Zhao, R. Scopelliti, E. E. Zvereva, S. A. Katsyuba and P. J. Dyson, *J. Phys. Chem. B*, 2007, **111**, 10095.
23 J. Pernak, K. Sobaszkiewicz and J. Foksowicz-Flaczyk, *Chem.–Eur. J.*, 2004, **10**, 3479.
24 L. C. Branco, J. N. Rosa, J. J. M. Ramos and C. A. M. Afonso, *Chem.–Eur. J.*, 2002, **8**, 3671.
25 Q. Liu, M. H. A. Janssen, F. v. Rantwijk and R. A. Sheldon, *Green Chem.*, 2005, **7**, 39.
26 M. Yoshizawa-Fujita, T. Tamura, Y. Takeoka and M. Rikukawa, *Chem. Commun*, 2011, **47**, 2345.
27 Z.-B. Zhou, H. Matsumoto and K. Tatsumi, *Chem.–Eur. J.*, 2005, **11**, 752.
28 T. Sato, G. Masuda and K. Takagi, *Electrochim. Acta*, 2004, **49**, 3603.
29 H. Matsumoto, H. Sakaebe and K. Tatsumi, *J. Power Sources*, 2005, **146**, 45.
30 C. M. Lang and P. A. Kohl, *J. Electrochem. Soc.*, 2007, **154**, F106.
31 P. Petiot, C. Charnay, J. Martinez, L. Puttergill, F. Galindo, F. Lamaty and E. Colacino, *Chem. Commun.*, 2010, **46**, 8842.
32 K. Tsunashima and M. Sugiya, *Electrochem. Commun.*, 2007, **9**, 2353.
33 J. Kim, R. P. Singh and J. M. Shreeve, *Inorg. Chem.*, 2004, **43**, 2960.

34 Z.-B. Zhou, H. Matsumoto and K. Tatsumi, *Chem.–Eur. J.*, 2006, **12**, 2196.
35 S. Fang, L. Yang, J. Wang, M. Li, K. Tachibana and K. Kamijim, *Electrochim. Acta*, 2009, **54**, 4269.
36 S. Fang, Y. Tang, X. Tai, L. Yang, K. Tachibana and K. Kamijima, *J. Power Sources*, 2011, **196**, 1433.
37 H.-B. Han, J. Nie, K. Liu, W.-K. Li, W.-F. Feng, M. Armand, H. Matsumoto and Z.-B. Zhou, *Electrochim. Acta*, 2010, **55**, 1221.
38 N. Terasawa, S. Tsuzuki, T. Umecky, Y. Saitoc and H. Matsumoto, *Chem. Commun.*, 2010, **46**, 1730.
39 S. S. Y. Tan and D. R. MacFarlane, *Top. Curr. Chem.*, 2009, **290**, 311.
40 H. Ohno and Y. Fukaya, *Chem. Lett.*, 2009, 2.
41 A. Stark, *Energy Environ. Sci.*, 2011, **4**, 19.
42 A. Corma, S. Iborra and A. Velty, *Chem. Rev.*, 2007, **107**, 2411.
43 P. L. Dhepe and A. Fukuoka, *ChemSusChem*, 2008, **1**, 969.
44 Y. Nishiyama, P. Langan and H. Chanzy, *J. Am. Chem. Soc.*, 2002, **124**, 9074.
45 S. Park, J. O. Baker, M. E. Himmel, P. A. Parilla and D. K. Johnson, *Biotechnol. Biofuels*, 2010, **3**, 10.
46 R. P. Swatloski, S. K. Spear, J. D. Holbrey and R. D. Rogers, *J. Am. Chem. Soc.*, 2002, **124**, 4974.
47 H. Zhang, J. Wu, J. Zhang and J. He, *Macromolecules*, 2005, **38**, 8272.
48 Y. Fukaya, K. Hayashi, M. Wadab and H. Ohno, *Green Chem.*, 2008, **10**, 44.
49 Y. Fukaya, A. Sugimoto and H. Ohno, *Biomacromolecules*, 2006, **7**, 3295.
50 Y. Cao, J. Wu, J. Zhang, H. Q. Li, Y. Zhang and J. S. He, *Chem. Eng. J.*, 2009, **147**, 13.
51 H. Liu, K. L. Sale, B. M. Holmes, B. A. Simmons and S. Singh, *J. Phys. Chem. B*, 2010, **114**, 4293.
52 A. Pinkert, K. N. Marsh, S. Pang and M. P. Staiger, *Chem. Rev.*, 2009, **109**, 6712.
53 J. B. Binder and R. T. Raines, *J. Am. Chem. Soc.*, 2009, **131**, 1979.
54 Y. Zhu, Z. N. Kong, L. P. Stubbs, H. Lin, S. Shen, E. V. Anslyn and J. A. Maguire, *ChemSusChem*, 2010, **3**, 67.
55 A. P. Abbott, T. J. Bell, S. Handa and B. Stoddart, *Green Chem.*, 2005, **7**, 705.
56 S. K. Mahadeva, K.-S. Kang, J. Kim, S. H. Ha and Y.-M. Koo, *Soft Mater.*, 2010, **8**, 254.
57 S.-J. Kim, A. A. Dwiatmoko, J. W. Choi, Y.-W. Suh, D. J. Suh and M. Oh, *Bioresour. Technol.*, 2010, **101**, 8273.
58 K. Shill, S. Padmanabhan, Q. Xin, J. M. Prausnitz, D. S. Clark and H. W. Blanch, *Biotechnol. Bioeng.*, 2011, **108**, 511.
59 K. Fujii, S. Seki, S. Fukuda, R. Kanzaki, T. Takamuku, Y. Umebayashi and S. Ishiguro, *J. Phys. Chem. B*, 2007, **111**, 12829.
60 J. M. Pringle, P. C. Howlett, D. R. MacFarlane and M. Forsyth, *J. Mater. Chem.*, 2010, **20**, 2056.
61 A. R. Katritzky, R. Jain, A. Lomaka, R. Petrukhin, U. Maran and M. Karelson, *Cryst. Growth Des.*, 2001, **1**, 261.
62 M. C. Kroon, W. Buijs, C. J. Peters and G.-J. Witkamp, *Thermochim. Acta*, 2007, **465**, 40.
63 H. Ohno, *Electrochemical Aspects of Ionic Liquids*, Wiley-Interscience, New York, 2005.
64 D. R. MacFarlane, P. Meakin, J. Sun, N. Amini and M. Forsyth, *J. Phys. Chem. B*, 1999, **103**, 4164.
65 P. Bonhôte, A.-P. Dias, N. Papageorgiou, K. Kalyanasundaram and M. Grätzel, *Inorg. Chem.*, 1996, **35**, 1168.
66 C. Zhao, G. Burrell, A. A. J. Torriero, F. Separovic, N. F. Dunlop, D. R. MacFarlane and A. M. Bond, *J. Phys. Chem. B*, 2008, **112**, 6923.
67 C. Reichardt, *Solvents and Solvent Effects in Organic Chemistry*, 3rd edn, VCH, Weinheim, 2003.
68 R. L. Gardas and J. A. P. Coutinho, *Fluid Phase Equilib.*, 2008, **266**, 195.
69 A. P. Abbott, *ChemPhysChem*, 2005, **6**, 2502.
70 A. S. Pensado, M. J. P. Comuñas and J. Fernández, *Tribol. Lett.*, 2008, **31**, 107; C. Schreiner, S. Zugmann, R. Hartl and H. J. Gores, *J. Chem. Eng. Data*, 2010, **55**, 4372.
71 J. Sun, M. Forsyth and D. R. MacFarlane, *J. Phys. Chem. B*, 1998, **102**, 8858.
72 Md. A. B. H. Susan, A. Noda, S. Mitsushima and M. Watanabe, *Chem. Commun.*, 2003, 938.
73 T. Heinze, K. Schwikal and S. Barthel, *Macromol. Biosci.*, 2005, **5**, 520.
74 Y. Wang and G. A. Voth, *J. Am. Chem. Soc.*, 2005, **127**, 12192.
75 Y. Wang, W. Jiang, T. Yan and G. A. Voth, *Acc. Chem. Res.*, 2007, **40**, 1193.
76 D. J. Gardner, G. S. Oporto, R. Mills and M. A. S. A. Samir, *J. Adhes. Sci. Technol.*, 2008, **22**, 55.
77 M. M. Chang, T. Y. C. Chou and G. T. Tsao, Structure, Pretreatment and Hydrolysis of Cellulose, *Adv. Biochem. Eng.*, 1981, **20**, 15.
78 I. S. Kim, J. P. Kim, S. Y. Kwak, Y. S. Ko and Y. K. Kwon, *Polymer*, 2006, **47**, 1333.
79 H. Meerwein, *Org. Synth.*, 1973, **Coll. Vol. 5**, 1080; H. Meerwein, *Org. Synth.*, 1966, **46**, 113.

